Lab on a Chip

PAPER

View Article Online
View Journal | View Issue

Cite this: *Lab Chip*, 2016, **16**, 2093

Embroidered electrochemical sensors for biomolecular detection†

Xiyuan Liu and Peter B. Lillehoj*

Electrochemical sensors are powerful analytical tools which possess the capacity for rapid detection of biomarkers in clinical specimens. While most electrochemical sensors are fabricated on rigid substrates, there is a growing need for sensors that can be manufactured on inexpensive and flexible materials. Here, we present a unique embroidered electrochemical sensor that is capable of quantitative analytical measurements using raw biofluid samples. Conductive threads immobilized with enzyme probes were generated using a simple and robust fabrication process and used to fabricate flexible, mechanically robust electrodes on textiles. For proof of concept, measurements were performed to detect glucose and lactate in buffer and whole blood samples, which exhibited excellent specificity and accuracy. We also demonstrate that our embroidered biosensor can be readily fabricated in two-dimensional (2D) arrays for multiplexed measurements. Lastly, we show that this biosensor exhibits good resiliency against mechanical stress and superior repeatability, which are important requirements for flexible sensor platforms.

Received 3rd March 2016,
Accepted 29th April 2016

DOI: 10.1039/c6lc00307a

www.rsc.org/loc

Introduction

Electrochemical sensors are a promising technology for analytical measurements due to their speed, small size, and high sensitivity.[1] Most commercial electrochemical sensors consist of screen-printed electrodes on rigid substrates such as glass or plastic.[2,3] However, the use of flexible materials offers several useful advantages for point-of-care testing including lower device costs and improved disposability, which are particularly important for use in resource-limited settings. Towards this end, researchers have developed screen-printed electrochemical sensors on plastic films[4–7] and paper.[8–10] While these platforms are promising, plastic typically requires surface modification for capillary flow and paper suffers from limited durability. Alternatively, textile is a widely available, inexpensive material that offers capillary-based sample transport and enhanced robustness compared with paper. Furthermore, textile-based sensors and electronics offer facile integration with wearable materials and garments which can be used to develop wearable sensor systems. Recent research in wearable sensing has focused on the integration of sensors onto fabrics for monitoring physiological parameters such as temperature,[11] heart rate[12,13] and respiration.[14] With respect to chemical sensing, Wang's group has developed electrochemical sensors on fabrics for health,[15] wound,[16] and environmental monitoring.[17,18] Diamond's group has also demonstrated wearable, textile-based electrochemical sensors for sweat analysis.[19,20] While these devices are capable of performing sensitive analytical measurements, they rely on screen-printed sensors which tend to be mechanically fragile and can be challenging to integrate with textile-based electronic components. Recently, a textile-based electrochemical sensor was reported which employs conductive silk yarn woven into the fabric.[21] This approach offers improved robustness compared with screen-printed sensors, but is limited to simple electrode geometries and substrates that are woven.

Here, we report for the first time an embroidered electrochemical sensor on textile for quantitative analytical measurements. This unique approach employs conductive thread which can be embroidered onto various types of textiles and fabrics. Using a computerized embroidery machine, electrodes can be quickly fabricated with customized geometries and configurations to accommodate commercial or custom electrochemical instrumentation. For wearable sensing applications, sensors can be embroidered at specific locations on a garment needed for sampling or detection. This technique is also amenable to high-volume production which minimizes device costs associated with *in vitro* diagnostic testing. Due to the hydrophilic nature of most threads, embroidered sensors can quickly absorb liquids facilitating sample loading and improving automation. To demonstrate the functionality of this biosensor technology for point-of-care testing, we performed several studies to evaluate its specificity and accuracy for the detection of glucose and lactate in

Department of Mechanical Engineering, Michigan State University, East Lansing, MI, USA. E-mail: lillehoj@egr.msu.edu

† Electronic supplementary information (ESI) available. See DOI: 10.1039/c6lc00307a

buffer and whole blood samples. We also show that our embroidered sensor can be used for multiplexed detection with high specificity and sensitivity by fabricating a sensor array for simultaneous measurements of analytes. Lastly, we evaluate the performance of our biosensor under repeated mechanical deformation, which reveals its ability to generate accurate and consistent measurements under such conditions.

Experimental

Biochemicals and reagents

Glucose, glucose oxidase, uric acid, and L-lactate were purchased from Sigma-Aldrich (St. Louis, MO) and lactate oxidase was purchased from A.G. Scientific (San Diego, CA). Silver/silver chloride (Ag/AgCl) and carbon inks were purchased from Conductive Compounds Inc. (Hudson, NH). Blocker Casein in PBS was purchased from Thermo Scientific (Tustin, CA). Deionized (DI) water was generated using a Barnstead Smart2Pure water purification system. For single and multi-analyte measurements in buffer samples, analytes were dissolved in PBS at room temperature. Blood samples were prepared by adding analytes in human whole blood from BioreclamationIVT (Hicksville, NY). Samples were freshly prepared prior to experiments and remaining biochemicals were used without further purification.

Thread preparation

The electrochemical sensors consist of three electrodes, a reference electrode (RE), working electrode (WE) and counter electrode (CE), which were fabricated from custom conductive thread. Briefly, polyester thread (Brothers International, Bridgewater, NJ) was coated with carbon or Ag/AgCl ink and cured at 120 °C for 40 min. Thread coated with carbon ink was used for the WE and CE, and thread coated with Ag/AgCl ink was used for the RE. For Ag/AgCl thread, soldering flux (Kester, Itasca, IL) was applied to the thread using a flux pen (Fig. S1a†) prior to the ink coating process to minimize oxidation of the ink. Glucose oxidase or lactate oxidase was immobilized onto the WE by immersing carbon-coated thread in either a glucose oxidase (645 U mL^{-1}) or lactate oxidase (256 U mL^{-1}) solution, followed by air drying overnight at room temperature.

Thread characterization

Threads were characterized using optical microscopy (Nikon Eclipse TS100-F trinocular microscope and DS-Fi1 camera), scanning electron microscopy (SEM) and energy-dispersive X-ray spectroscopy (EDS) to study their morphology after the ink coating process. SEM images and EDS spectrum were captured using a JEOL 6620LV scanning electron microscope at 10 kV or 12 kV with 1200× and 170× magnifications for Fig. 1c and d, respectively. The electrical properties of the threads were characterized by measuring their electrical resistance using a Fluke 87-V digital multimeter. Threads were cut into 1 m-long pieces and attached to the multimeter by clamping the ends using alligator clip probes (Fig. S1b†).

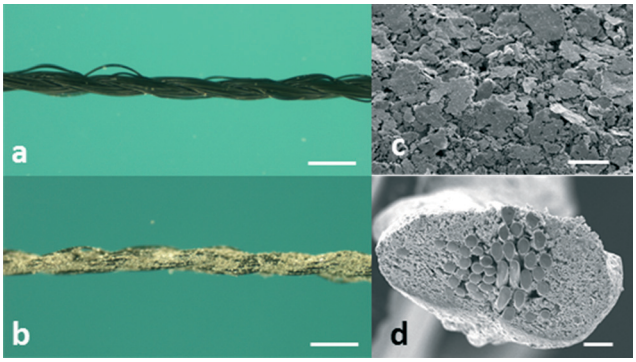

Fig. 1 Optical images of uncoated thread (a) and Ag/AgCl-coated thread (b). Scale bar, 500 μm. SEM images of Ag/AgCl-coated thread showing its surface morphology (c) and cross-section (d). Scale bar, 50 μm.

Sensor design and fabrication

Electrodes were designed using AutoCAD software (Autodesk, Vernon Hills, IL) and converted into an embroidery file using SewArt software (S & S Computing). Several embroidery parameters, such as the stitch length and stitch density, were optimized to enhance the embroidery quality for improved signal consistency and signal-to-noise ratio (SNR). The electrodes were fabricated using a Brothers SE400 computerized embroidery machine on polyester fabric stacked with an embroidery stabilizer film (World Weidner, Ponca City, OK). After the sensors were embroidered, the stabilizer film was removed and individual sensors were cut and stored at ambient conditions prior to experiments.

Electrochemical measurements

Amperometric measurements were performed using a multichannel electrochemical workstation (GeneFluidics, Inc. Irwindale, CA). For single analyte measurements, 35 μL of sample was dispensed onto the sensing region using a pipette, followed by the application of a −200 mV bias potential after 1 min. For multi-analyte measurements, 60 μL of sample was used. All measurements were performed at room temperature under ambient conditions using new sensors.

Results and discussion

Characterization of ink-coated thread

Optical images of uncoated thread (Fig. 1a) and Ag/AgCl-coated thread (Fig. 1b) show the effects of the thread coating and enzyme immobilization process. As shown in Fig. 1b, the entire length of thread is uniformly coated with Ag/AgCl with negligible blotching or defects. Similar surface coverage was also observed for carbon-coated thread. SEM was used to further observe changes in the thread surface morphology following the coating process. Magnified images of Ag/AgCl-coated thread reveal that Ag/AgCl completely fills the microscopic voids on the surface thereby improving surface coverage (Fig. 1c). Cross-sectional images of the threads show that Ag/AgCl permeates into the fibers at depths of up to 50 μm

(Fig. 1d), which is confirmed by EDS analysis (Fig. S2†). These results also demonstrate that the enzyme immobilization process has a negligible impact on the surface morphology and the coating thickness. Since the electrical properties of the threads are strongly dependent on the quality of the ink coating, we also measured the electrical resistance of the coated threads. Ag/AgCl and carbon-coated thread exhibited resistances of ~0.8 and ~140 Ω cm^{-1} respectively, which is similar to values reported in literature.[21] The resistance of Ag/AgCl-coated thread was significantly reduced by applying flux to the thread which helped to prevent oxidation of Ag/AgCl. The resistance of Ag/AgCl-coated thread without flux can reach as high as 80 Ω cm^{-1}.

Thread embroidery characterization

Embroidery is an intricate process where graphical patterns are sewn onto fabrics using thread. Several embroidery parameters, including stitch length and separation distance, were studied to optimize the quality of the electrodes. For instance, decreasing the stitch separation distance resulted in a higher stitch density which improved electrode uniformity. However, using a higher stitch density required a larger amount of thread which increased the electrical resistance of the electrodes. We determined that a stitch separation distance of 0.2 mm and stitch length of 0.5 mm produced consistent uniformity while minimizing the electrode resistance. Using these optimized parameters, we successfully fabricated sensors and sensor arrays onto polyester and cotton fabrics, as well as garments. Fig. 2 shows proof-of-concept examples of embroidered sensors on a textile "chip" for *in vitro* diagnostic testing, a cotton gauze for wound monitoring and a cotton t-shirt for sweat analysis.

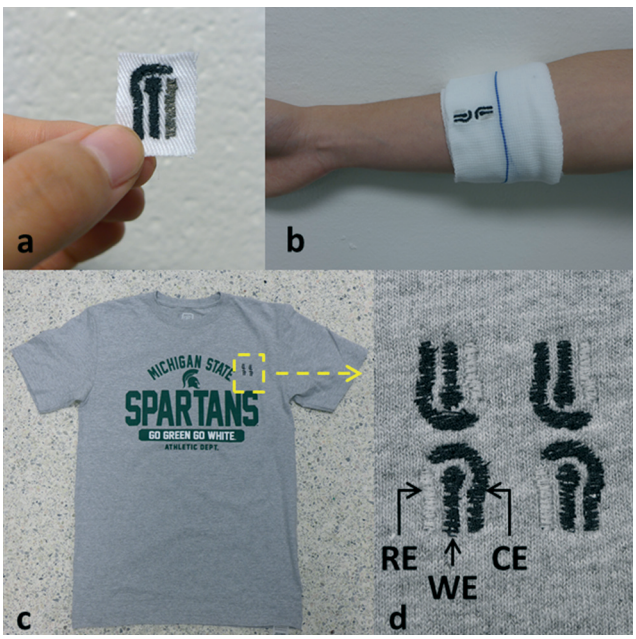

Fig. 2 Embroidered electrochemical sensors fabricated on a textile "chip" (a), cotton gauze (b) and cotton t-shirt (c). Zoomed-in image of the sensor array on the t-shirt (d).

Single analyte detection

To demonstrate the utility of this technology for quantitative biomarker detection, we first performed measurements of glucose in buffer samples. 35 μL of sample was dispensed onto the sensing area, as shown in Fig. 3a, which was quickly soaked up by the electrodes due to the high wettability of the thread and fabric. Measurements were performed after 1 min, which was sufficient time for the sample to be fully absorbed and generate a stable electrochemical reaction. The glucose assay exhibits a highly linear response over the entire concentration range with a R^2 correlation coefficient of 0.996 (Fig. 3b). In addition, it exhibits very low background noise at 0 mM and very small standard deviations (SDs) of <3% over three individual measurements obtained using new sensors, which demonstrates the high accuracy and reproducibility of this assay. Measurements were also performed to detect lactate in buffer samples using sensors functionalized with lactate oxidase. Similar to the glucose assay, this assay exhibits an excellent linear response over the entire concentration range (R^2 = 0.992) and highly accurate measurements with SDs of <6% (Fig. 3c). These results show that our embroidered biosensor can quickly and accurately detect different types of analytes on a flexible, textile platform.

Multiplexed detection

In addition to single analyte measurements, experiments were carried out using our embroidered biosensors for multiplexed measurements of glucose and lactate. We first tested the specificity of the individual glucose and lactate assays by performing measurements using a mixture of analytes in PBS including glucose (5 mM), lactate (12.5 mM) and uric acid (40 mM). For the glucose assay, only the glucose sample generated a significant response (SNR of 3.2) compared with the irrelevant targets and blank control (Fig. 4b). Similarly, the lactate assay only generated a substantial response to lactate (SNR of 4.1) with negligible signals from the nonspecific analytes (Fig. 4c). These results indicate that our sensor is capable of high specificity measurements and suitable for multiplexed detection of multiple analytes with a low likelihood of interference caused by nonspecific targets.

We designed a dual electrochemical sensor, with two sensors facing opposite to each other (Fig. 4a), for simultaneous measurements of glucose and lactate. One sensor was functionalized with glucose oxidase and the other was functionalized with lactate oxidase. Using this dual sensor, we first tested a sample containing only 40 mM of glucose. As shown in Fig. 4d, only the glucose oxidase-functionalized sensor generated a significant signal, which is consistent with the results from the individual assay measurements in Fig. 4b. In contrast, the lactate oxidase-functionalized sensor generated a negligible signal similar to that of the PBS blank control. We also tested a 50 mM lactate sample using the dual sensor and only the lactate oxidase-functionalized sensor generated

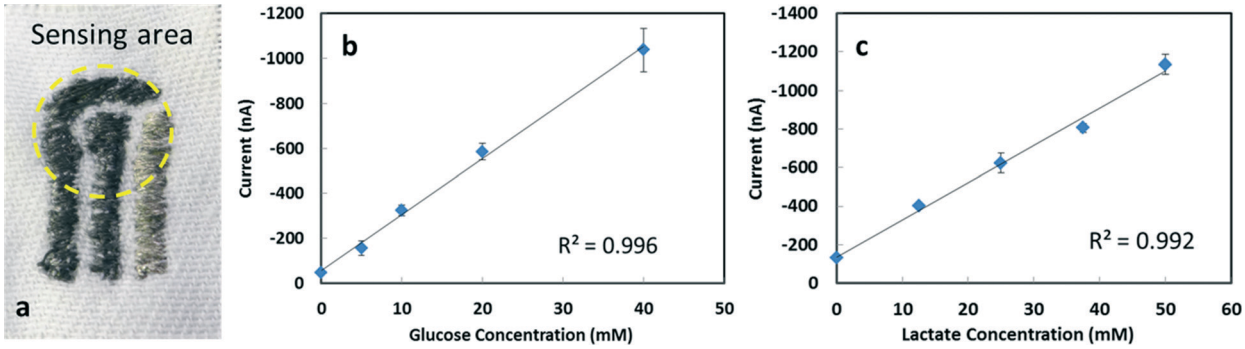

Fig. 3 (a) Close-up image of a single embroidered electrochemical sensor. The yellow dashed circle represents the sensing area. Amperometric measurements of glucose (b) and lactate (c) in buffer. Values are averaged over the final 10 s of the detection signal. Each data point represents the mean ± standard deviation (SD) of three separate measurements which were obtained using new sensors.

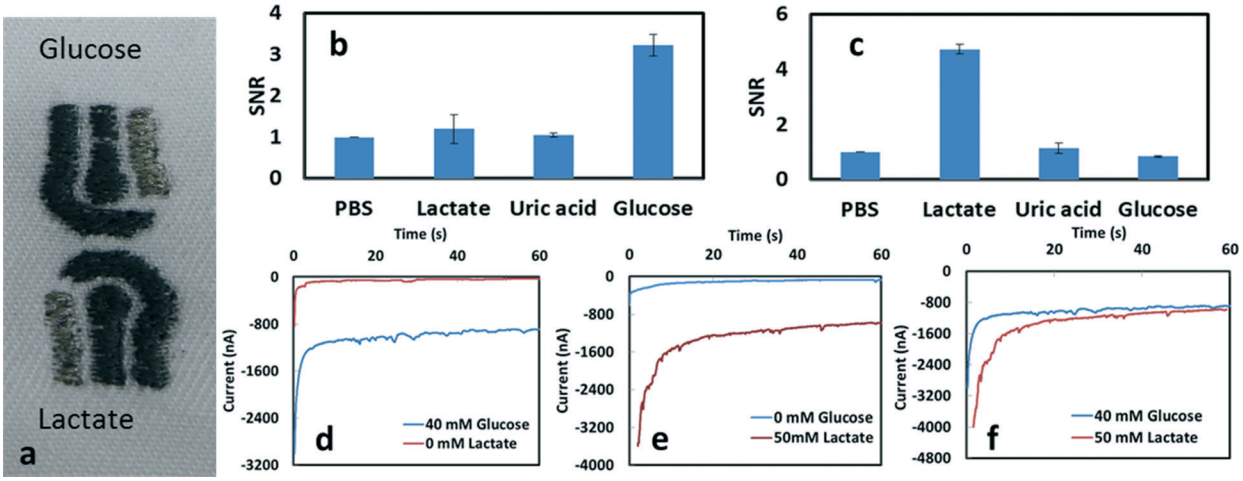

Fig. 4 (a) Close-up image of a dual electrochemical sensor for multiplexed analyte detection. Specificity of the glucose assay (b) and lactate assay (c) using glucose (5 mM), lactate (12.5 mM) and uric acid (40 mM) in PBS, and PBS (blank). Amperometric signals of a 40 mM glucose sample (d), 50 mM lactate sample (e) and 40 mM glucose + 50 mM lactate sample (f) using the dual electrochemical sensor. Each bar represents the mean ± SD of three separate measurements which were obtained using new sensors.

a significance response (Fig. 4e), demonstrating the high specificity of our dual electrochemical sensor.

For multiplexed detection, we prepared a sample containing 40 mM glucose and 50 mM lactate and dispensed it onto the dual sensor chip. Two distinct signals were simultaneously generated corresponding to the glucose and lactate targets (Fig. 4f). These collective results show that the signals generated for different analytes do not interfere with each other during multiplexed measurements. By incorporating additional sensors in the array, it will be possible to perform simultaneous measurements of numerous analytes from a single sample. While the dual electrochemical sensor used in this work was designed to accommodate our electrochemical analyzer, it is possible to design sensor arrays that can accommodate other commercial or custom electrochemical instrumentation.

Glucose detection in whole blood

To further demonstrate the utility of this sensor for biomolecular detection, we tested its performance for analyte measurements in whole blood. Blood samples spiked with glucose were dispensed on the sensor and placed in the electrochemical reader (Fig. 5a). Due to the higher viscosity of blood compared with buffer, it took slightly longer (~30 s) for the sample to completely be absorbed by the electrodes. Similar to glucose measurements in PBS, this assay exhibits a highly linear response (R^2 = 0.992) from 0 mM to 40 mM (Fig. 5b), which spans the clinically relevant blood glucose concentrations in humans. Additionally, the low detection signal at 0 mM indicates that this assay generates minimal background noise even in complex biological matrices. These results show that our embroidered sensor is capable of accurate quantitative measurements of protein biomarkers in clinical samples and holds great potential for point-of-care testing.

Sensor durability testing

An important consideration for flexible sensors is the influence of mechanical deformation on the detection performance. Specifically, textile sensors are inherently susceptible to deformation (*i.e.* bending or folding) before and during

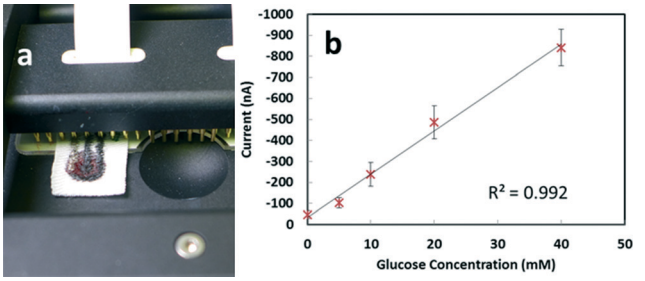

Fig. 5 (a) Embroidered sensor inside the electrochemical workstation during testing. (b) Amperometric measurements of glucose in whole blood. Values are averaged over the final 10 s of the detection signal. Each data point represents the mean ± SD of three separate measurements which were obtained using new sensors.

testing and should be able to maintain detection accuracy. To mimic such effects, we carried out two studies using our embroidered biosensor. In the first study, we manually folded and flattened the sensor (as shown in Fig. 6a) for up to 100 cycles, and performed measurements of lactate samples at intervals of 5, 10, 25, 50 and 100 bending cycles. By comparing the signals of sensors that underwent bending with control sensors that did not undergo deformation (Fig. 6b), we can see that there is negligible change in the signal after 25 cycles, which is a reasonable limit for *in vitro* diagnostic testing. Furthermore, there is only a marginal decrease of 7% and 9% in the signal after 50 and 100 cycles, respectively, which is tolerable for wearable sensing applications.

In the second study, we examined the sensor performance in response to deformation occurring simultaneously while the measurement was being carried out. To experimentally mimic this scenario, we performed measurements of lactate

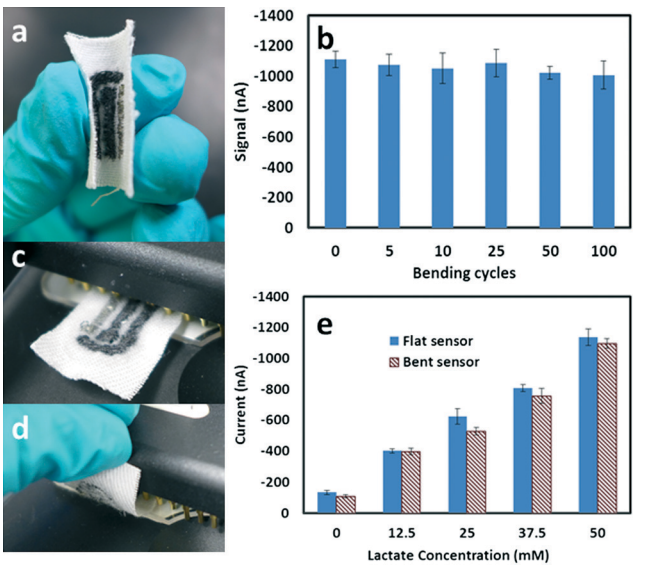

Fig. 6 (a) Mechanical bend testing of embroidered electrochemical sensors. (b) Amperometric measurements of lactate (50 mM) in PBS following up to 100 cycles of bending. Images of the sensor positioned flat (c) and bent at 90° (d) in the reader. (e) Comparative measurements of lactate using flat or bent sensors. Each bar represents the mean ± SD of three separate measurements.

samples (0–50 mM) using sensors which were manually bent at 90° while the signals were being recorded. Comparative signals from sensors positioned flat in the reader (Fig. 6c) and mechanically bent sensors (Fig. 6d) are shown in Fig. 6e. While the signal of the bent sensors slightly diminishes at concentrations above 25 mM, the signal maintains a highly linear response (R^2 = 0.981) throughout the tested concentration range, which is similar to that of the flat sensor. Additionally, both the bent and flat sensors exhibit high accuracy as represented by the low SD (<6%) of multiple measurements. These data reveal that mechanical deformation during testing has a minimal impact on the performance of our embroidered biosensor as the response from the bent sensors is nearly identical to those from the flat sensors. These results also suggest that our embroidered biosensor will be able to maintain its accuracy and reproducibly under instances of repeated deformation for *in vitro* diagnostic testing or wearable sensing.

Conclusions

We report the first demonstration of an embroidered electrochemical sensor for quantitative biomarker measurements. This biosensor consists of electrodes fabricated from conductive threads that are subsequently embroidered onto wearable fabrics. Based on this approach, biosensor arrays can be rapidly produced with customized electrode geometries and configurations. For proof of concept, we performed single analyte measurements of glucose and lactate in PBS, which exhibited high specificity, a highly linear response and excellent accuracy. A dual sensor was fabricated and employed for multiplexed measurements of glucose and lactate, which exhibited similar performance as our single analyte assays. We further demonstrated the utility of this platform for biomolecular detection by using it for glucose measurements in whole blood samples, which exhibited excellent performance, thereby showcasing its usefulness for clinical sample testing. Experiments to evaluate the performance of our biosensor in response to mechanical deformation showed its capability to produce consistent and accurate measurement in response to repeated folding/bending prior to and during testing. In addition to its exceptional sensing performance, our embroidered biosensor is amenable to high-volume production using existing manufacturing technologies which minimizes overall costs and enables facile integration with inexpensive and wearable materials. These collective features make our embroidered electrochemical sensors well suited for diagnostic applications requiring rapid, accurate measurements on disposable and wearable platforms. For wearable sensing applications, we envision that our sensors could be integrated with miniature sensing electronics on textiles using conductive ink or thread, and data could be transmitted wirelessly to a peripheral device (*e.g.* a smartphone).[16,22] Further advancements in electronic textiles (e-textiles) may also enable electronics to be directly integrated into garments thereby improving device portability and user comfort.[23]

Acknowledgements

This work was supported by the National Science Foundation CAREER award (ECCS-135056). We thank Ying-Hung (Michelle) Lou and Evelynne Pyne for assisting with early prototype development.

References

1 J. Wang, *Biosens. Bioelectron.*, 2006, **21**, 1887–1892.
2 I. Palchetti, A. Cagnini, M. Del Carlo, C. Coppi, M. Mascini and A. P. F. Turner, *Anal. Chim. Acta*, 1997, **337**, 315–321.
3 S. D. Sprules, J. P. Hart, S. A. Wring and R. Pittson, *Anal. Chim. Acta*, 1995, **304**, 17–24.
4 A. de la Escosura-Muñiz, M. Espinoza-Castañeda, M. Hasegawa, L. Philippe and A. Merkoçi, *Nano Res.*, 2014, **8**, 1180–1188.
5 R. F. Carvalhal, D. S. Machado, R. K. Mendes, A. L. J. Almeida, N. H. Moreira, M. H. O. Piazetta, A. L. Gobbi and L. T. Kubota, *Biosens. Bioelectron.*, 2010, **25**, 2200–2204.
6 B. Wang, J. Zhang and S. Dong, *Biosens. Bioelectron.*, 2000, **15**, 397–402.
7 H. Yin, Y. Zhou, J. Xu, S. Ai, L. Cui and L. Zhu, *Anal. Chim. Acta*, 2010, **659**, 144–150.
8 Z. Nie, C. A. Nijhuis, J. Gong, X. Chen, A. Kumachev, A. W. Martinez, M. Narovlyansky and G. M. Whitesides, *Lab Chip*, 2010, **10**, 477.
9 X. Liu and P. B. Lillehoj, *J. Lab. Autom.*, 2015, 2211068215573662.
10 W. Dungchai, O. Chailapakul and C. S. Henry, *Anal. Chem.*, 2009, **81**, 5821–5826.
11 M. Sibinski, M. Jakubowska and M. Sloma, *Sensors*, 2010, **10**, 7934–7946.
12 R. Paradiso, G. Loriga and N. Taccini, *IEEE Trans. Inf. Technol. Biomed.*, 2005, **9**, 337–344.
13 G. Loriga, N. Taccini, D. De Rossi and R. Paradiso, in *27th Annual International Conference of the Engineering in Medicine and Biology Society, 2005, IEEE-EMBS 2005*, 2005, pp. 7349–7352.
14 S. Jung, T. Ji and V. K. Varadan, *Smart Mater. Struct.*, 2006, **15**, 1872.
15 Y.-L. Yang, M.-C. Chuang, S.-L. Lou and J. Wang, *Analyst*, 2010, **135**, 1230–1234.
16 P. Kassal, J. Kim, R. Kumar, W. R. de Araujo, I. M. Steinberg, M. D. Steinberg and J. Wang, *Electrochem. Commun.*, 2015, **56**, 6–10.
17 M.-C. Chuang, J. R. Windmiller, P. Santhosh, G. V. Ramírez, M. Galik, T.-Y. Chou and J. Wang, *Electroanalysis*, 2010, **22**, 2511–2518.
18 K. Malzahn, J. R. Windmiller, G. Valdés-Ramírez, M. J. Schöning and J. Wang, *Analyst*, 2011, **136**, 2912.
19 B. Schazmann, D. Morris, C. Slater, S. Beirne, C. Fay, R. Reuveny, N. Moyna and D. Diamond, *Anal. Methods*, 2010, **2**, 342–348.
20 S. Coyle, K.-T. Lau, N. Moyna, D. O'Gorman, D. Diamond, F. Di Francesco, D. Costanzo, P. Salvo, M. G. Trivella, D. E. De Rossi, N. Taccini, R. Paradiso, J.-A. Porchet, A. Ridolfi, J. Luprano, C. Chuzel, T. Lanier, F. Revol-Cavalier, S. Schoumacker, V. Mourier, I. Chartier, R. Convert, H. De-Moncuit and C. Bini, *IEEE Trans. Inf. Technol. Biomed.*, 2010, **14**, 364–370.
21 T. Choudhary, G. P. Rajamanickam and D. Dendukuri, *Lab Chip*, 2015, **15**, 2064–2072.
22 Y.-D. Lee and W.-Y. Chung, *Sens. Actuators, B*, 2009, **140**, 390–395.
23 E. R. Post, M. Orth, P. R. Russo and N. Gershenfeld, *IBM Syst. J.*, 2000, **39**, 840–860.

